

Time Dependent Partial Waves and Vortex Rings in the Dynamics of Wave Packets*

R. Arvieu^a, P. Rozmej^b and W. Berek^b

^a Institut des Sciences Nucléaires, F 38026 Grenoble-Cedex, France
arvieu@frcpn11.in2p3.fr

^b Theoretical Physics Department, University MCS, 20-031 Lublin, Poland
rozmej@tytan.umcs.lublin.pl

February 13, 1997

Abstract

We have found a new class of time dependent partial waves which are solutions of time dependent Schrödinger equation for three dimensional harmonic oscillator. We also showed the decomposition of coherent states of harmonic oscillator into these partial waves. This decomposition appears particularly convenient for a description of the dynamics of a wave packet representing a particle with spin when the spin-orbit interaction is present in the hamiltonian. An example of an evolution of a localized wave packet into a torus and backwards, for a particular initial conditions is analysed in analytical terms and shown with a computer graphics.

PACS number(s): 03.65.Ge, 32.90+a

1 Introduction

The rapid technological development of short-pulsed lasers during the last decade made it possible to produce and detect particular states, coherent superpositions of stationary electron states for a wide variety of physical systems. The dynamics of these initially well localized wave packets is a subject of much current investigation in many areas of physics and chemistry [1, 2]. An extensive research by means of both theoretical and experimental methods has brought an understanding of the intriguing phenomena of a hierarchy of collapses and revivals for particularly prepared wave packets in Jaynes-Cummings Model (JCM) of quantum optics [3-7] and in Rydberg atoms [8-14].

In present paper we construct new solutions of time dependent Schrödinger equation for spherical harmonic oscillator (HO). We use these solutions further for description of the

*submitted to J. Phys. A

evolution of wave packets representing a particle with spin moving in HO potential with additional spin-orbit interaction. Time dependent partial waves allow for much clearer interpretation of subtle interference effects as well as for a substantial acceleration of numerical codes used for graphical presentation of a complicated wave packet motion.

The paper is organized as follows. In section 2 we construct time dependent partial waves for the harmonic oscillator and show the decomposition of coherent states into these states. In section 3 we show the motion of individual partial waves. In section 4 we discuss time dependent spinors corresponding to solutions of time dependent Schrödinger equation for hamiltonian containing spin-orbit interaction and show a possibility of evolution of an initially localized wave packet into a toroidal shape and backwards. Sections 5 and 6 present graphical illustrations of the wave packet motion and conclusions.

2 Time dependent partial waves for the harmonic oscillator

It is not so well known that there exist simple time dependent partial waves which are solutions of the Schrödinger equation of the three dimensional oscillator. The proof will be given below.

We look for solutions $\psi_l^m(\vec{r}, t)$ of the time dependent Schrödinger equation for the spherical harmonic oscillator (with $\hbar = m = \omega = 1$) with the following form

$$\psi_l^m(\vec{r}, t) = F(t) e^{-\frac{1}{2}r^2} W_l(R_0 e^{-it} r) Y_l^m(\theta, \varphi) \quad (1)$$

where $F(t)$ and W_l must be determined in terms of a complex number R_0 .

We find easily that W_l must obey the differential equation

$$Z^2 \frac{d^2 W_l}{dZ^2} + 2Z \frac{dW_l}{dZ} - [l(l+1) + (3 - \frac{2i}{F} \frac{dF}{dt}) r^2] W_l = 0 \quad (2)$$

with a new variable Z

$$Z = R_0 e^{-it} r. \quad (3)$$

W_l depends only on this variable if F solves the equation

$$3 - \frac{2i}{F} \frac{dF}{dt} = R_0^2 e^{-2it}. \quad (4)$$

Within an arbitrary constant factor, which is not written the solution is

$$F(t) = e^{-\frac{3}{2}it} e^{-\frac{1}{4}R_0^2 e^{-2it}}. \quad (5)$$

The equation solved by W_l becomes

$$Z^2 \frac{d^2 W_l}{dZ^2} + 2Z \frac{dW_l}{dZ} - [l(l+1) + Z^2] W_l = 0 \quad (6)$$

which is the equation for the modified spherical Bessel functions.

In the following we will use only the modified spherical Bessel functions of the first kind with the usual conventions of the literature [15]

$$W_l(Z) = \sqrt{\frac{\pi}{2Z}} I_{l+\frac{1}{2}}(Z) \quad (7)$$

$$= \frac{Z^l}{(2l+1)!!} \left[1 + \frac{\frac{1}{2}Z^2}{1!(2l+3)} + \frac{(\frac{1}{2}Z^2)^2}{2!(2l+3)(2l+5)} + \dots \right]. \quad (8)$$

The interpretation of these waves is very simple: there is an harmonic motion in the radial part of the wave function keeping the angular part the same because of angular momentum conservation.

The partial waves $\psi_l^m(\vec{r}, t)$ just defined occur in a natural way in the expansion of a coherent time dependent gaussian wave packet into partial waves. In such a wave packet the constant R_0 finds its interpretation by combining the position of the center of the wave packet \vec{r}_0 to its mean momentum \vec{p}_0 at a time $t = 0$. Let \vec{r}_t and \vec{p}_t be such vectors at time t and let us define

$$\vec{R}_t = \vec{r}_t + i\vec{p}_t, \quad (9)$$

while

$$\vec{R}_0 = \vec{r}_0 + i\vec{p}_0. \quad (10)$$

These two vectors are related by

$$\vec{R}_t = \vec{R}_0 e^{-it}. \quad (11)$$

A normalized gaussian wave packet centered on \vec{r}_t with mean momentum \vec{p}_t is now written as

$$\bar{\psi}_{\vec{R}_t}(\vec{r}) = \pi^{-\frac{3}{4}} e^{-\frac{1}{2}(\vec{r}-\vec{r}_t)^2} e^{i\vec{p}_t \cdot \vec{r}} = \pi^{-\frac{3}{4}} e^{-\frac{1}{2}r^2} e^{-\frac{1}{2}r_t^2} e^{\vec{r} \cdot \vec{R}_t}. \quad (12)$$

Using 10.2.36 from reference [15] the modified Bessel function of the first kind of argument $Z = R_t r = R_0 e^{-it} r$ appears in the expansion of the last exponential of (12)

$$e^{\vec{r} \cdot \vec{R}_t} = \sum_{l=0}^{\infty} (2l+1) \sqrt{\frac{\pi}{2Z}} I_{l+\frac{1}{2}}(Z) P_l(\cos \Theta) \quad (13)$$

and R_0 is defined as

$$R_0 = (\vec{R}_0 \cdot \vec{R}_0)^{\frac{1}{2}} = (r_0^2 - p_0^2 + 2i\vec{r}_0 \cdot \vec{p}_0)^{\frac{1}{2}}. \quad (14)$$

In a gaussian wave packet all the time dependent partial waves share the same parameter R_0 . However it is possible to consider more general wave packet for which R_0 might be different for different l .

The Legendre polynomial $P_l(\cos \Theta)$ depends on the (complex) angle Θ between \vec{r} and \vec{R}_t . However this angle is time independent. Indeed for each direction α , $\alpha = x, y, z$ one has

$$r_\alpha(t) + ip_\alpha(t) = (r_\alpha(0) + ip_\alpha(0)) e^{-it} \quad (15)$$

as well as equation (11), therefore

$$\begin{aligned} \cos(\Theta) &= \frac{x[x(t) + ip_x(t)] + y[y(t) + ip_y(t)] + z[z(t) + ip_z(t)]}{R_t r} \\ &= \frac{x[x(0) + ip_x(0)] + y[y(0) + ip_y(0)] + z[z(0) + ip_z(0)]}{R_0 r}. \end{aligned} \quad (16)$$

Then if the complex direction θ_{R_0} , φ_{R_0} of \vec{R}_0 is introduced through

$$\begin{aligned}\cos \theta_{R_0} &= \frac{z(0) + ip_z(0)}{R_0} \\ \sin \theta_{R_0} \cos \varphi_{R_0} &= \frac{x(0) + ip_x(0)}{R_0} \\ \sin \theta_{R_0} \sin \varphi_{R_0} &= \frac{y(0) + ip_y(0)}{R_0}\end{aligned}\tag{17}$$

one writes the addition formula:

$$P_l(\cos \Theta) = \frac{4\pi}{2l+1} \sum_{m=-l}^l (-1)^m Y_l^m(\theta, \varphi) Y_l^{-m}(\theta_{R_0}, \varphi_{R_0}).\tag{18}$$

We can now rewrite $\bar{\psi}_{\vec{R}_t}$ as

$$\bar{\psi}_{\vec{R}_t}(\vec{r}) = 4\pi^{\frac{1}{4}} e^{-\frac{1}{2}(r^2+r_t^2)} \sum_{l=0}^{\infty} \sum_{m=-l}^l (-1)^m Y_l^{-m}(\theta_{R_0}, \varphi_{R_0}) W_l(R_t r) Y_l^m(\theta, \varphi).\tag{19}$$

We will now extract the function F (5) in order to show explicitly the time dependent partial waves

$$\begin{aligned}e^{-\frac{1}{4}R_0^2} e^{-2it} &= e^{-\frac{1}{4}(r_t^2-p_t^2+2i\vec{r}_t \cdot \vec{p}_t)} \\ &= e^{-\frac{1}{2}r_t^2} e^{-\frac{i}{2}\vec{r}_t \cdot \vec{p}_t} e^{\frac{E_0}{2}}.\end{aligned}\tag{20}$$

The classical energy $E_0 = \frac{r_0^2+p_0^2}{2}$ has been introduced above. The time dependent partial waves (1) which appear in the gaussian wave packet at time t are then expressed as:

$$\psi_l^m(\vec{r}, t) = e^{-\left(\frac{3}{2}it + \frac{i}{2}\vec{r}_t \cdot \vec{p}_t + \frac{r^2+r_t^2}{2} - \frac{E_0}{2}\right)} W_l(R_t r) Y_l^m(\theta, \varphi).\tag{21}$$

The gaussian wave packet (19) can now be expressed as follows in terms of (21)

$$\bar{\psi}_{\vec{R}_t}(\vec{r}) = 4\pi^{\frac{1}{4}} e^{i\left(\frac{3}{2}t + \frac{\vec{r}_t \cdot \vec{p}_t}{2}\right) - \frac{E_0}{2}} \sum_{lm} (-1)^m Y_l^{-m}(\theta_{R_0}, \varphi_{R_0}) \psi_l^m(\vec{r}, t).\tag{22}$$

Clearly one obtains a solution of the Schrödinger equation only if we change the phase. Let $\psi_{\vec{R}_t}(\vec{r})$ be this solution

$$\begin{aligned}\psi_{\vec{R}_t}(\vec{r}) &= e^{-i\left(\frac{3}{2}t + \frac{\vec{r}_t \cdot \vec{p}_t}{2}\right)} \bar{\psi}_{\vec{R}_t}(\vec{r}) \\ &= \sum_{lm} (-1)^m 4\pi^{\frac{1}{4}} e^{-\frac{E_0}{2}} Y_l^{-m}(\theta_{R_0}, \varphi_{R_0}) \psi_l^m(\vec{r}, t) \\ &= \sum_{lm} C_{lm}(\vec{R}_0) \psi_l^m(\vec{r}, t).\end{aligned}\tag{23}$$

The weight $C_{lm}(\vec{R}_0)$ of the time dependent partial wave $\psi_l^m(\vec{r}, t)$ is now seen to be

$$C_{lm}(\vec{R}_0) = (-1)^m 4\pi^{\frac{1}{4}} e^{-\frac{E_0}{2}} Y_l^{-m}(\theta_{R_0}, \varphi_{R_0}).\tag{24}$$

An expansion similar to equation (23) is found in reference [16]. However the time dependence of the radial function is lacking in this reference as well as the phase which is needed to correct the gaussian wave packet. The existence of this phase is mentioned in some textbooks [17].

3 Representation of the time dependent partial waves

Let us define the phase of R_0 by

$$R_0 = (r_0^2 - p_0^2 + 2i\vec{r}_0 \cdot \vec{p}_0)^{\frac{1}{2}} = |R_0| e^{i\delta_0}. \quad (25)$$

The argument of the modified Bessel function is $Z = r|R_0|e^{-i(t-\delta_0)}$. Changing the initial conditions of the wave packet produces a change of $|R_0|$ and of δ_0 . However it is clear that the change of the phase can be taken into account in the radial partial wave $W_l(z)$ by a shift of the origin of time. It is therefore possible to analyse the different partial waves by assuming that $\delta_0 = 0$. This possibility arises if $p_0 = 0$, $R_0 = r_0$. For these values the gaussian wave packet performs a linear motion. It is striking that the radial motions of the partial waves corresponding to such a case contain all the proper information which can be used for all the different trajectories, i.e. circular or elliptical. The differences between the trajectories will be introduced by the coefficients $C_{lm}(\vec{R}_0)$.

In the following figures we have chosen to study the radial waves for the mean energy $E_0 = N = 20$ i.e. $r_0 = \sqrt{2E_0} = \sqrt{40} = R_0$. The 8 lowest partial waves present in the development of a gaussian wave packet are represented in figure 1 [as a matter of fact we have represented the density multiplied by r^2] for a time range going from $t = 0$ to $\frac{T}{2}$ (T is the harmonic oscillator period). The densities exhibit the same motion toward the origin and of course this radial motion is symmetric with respect to $t = \frac{T}{4}$. However there is clearly an effect of the centrifugal barrier since the waves with the highest l are repelled from the origin. Also some secondary maxima are present. It is worth to mention once again that the effects of the centrifugal barrier cancel when one adds the waves to produce a linear motion. We should also note that the spread of the partial waves does not depend on l in a significant manner.

In figure 2 the squares of 16 lowest partial waves ($|r\psi_l(r, t)|^2$) are represented as functions of r for $t = 0$. The concentration of the waves at the same r is spectacular. The intensity of the waves increases when l goes from $l = 0$ to $l = 4$ and decrease afterwards. In order to explain the concentration of the wave in three dimensions the angular part plays a role as will be discussed later on.

4 Time dependent spinors

We will now study the evolution of a coherent wave packet which is initially in a pure spin eigenstate chosen as $s_z = +\frac{1}{2}$. This wave packet will evolve on the action of the harmonic oscillator evolution operator $U_0(t)$ and of the spin-orbit part $U_{ls}(t)$. As in our previous papers [18–22] we will use the spin-orbit hamiltonian with a constant factor κ :

$$V_{ls} = \kappa (\vec{l} \cdot \vec{\sigma}) \quad (26)$$

and therefore U_0 commute with V_{ls} . The hamiltonian contains the ratio of the two time scales (let us recall that $\omega = 1$)

$$\frac{T_{ls}}{T} = \frac{2\pi}{\kappa} \frac{\omega}{2\pi} = \frac{1}{\kappa}. \quad (27)$$

The fully normalized spinor is written at time $t = 0$ as

$$\tilde{\psi}_{\vec{R}_0}(\vec{r}) = \begin{pmatrix} \psi_{\vec{R}_0}(\vec{r}) \\ 0 \end{pmatrix} = \sum_{lm} C_{lm}(\vec{R}_0) \begin{pmatrix} \psi_l^m(\vec{r}, 0) \\ 0 \end{pmatrix}. \quad (28)$$

We have shown previously [4] that

$$U_{ls}(t) = f(t) + g(t) (\vec{l} \cdot \vec{\sigma}) \quad (29)$$

with the following operators

$$f(t) = e^{i\frac{t}{2}} \left(\cos \Omega \frac{t}{2} - \frac{1}{\Omega} \sin \Omega \frac{t}{2} \right) \quad (30)$$

$$g(t) = e^{i\frac{t}{2}} \left(-\frac{2i}{\Omega} \sin \Omega \frac{t}{2} \right) \quad (31)$$

$$\Omega |lm\rangle = \sqrt{1 + 4\hat{l}^2} |lm\rangle = (2l + 1) |lm\rangle. \quad (32)$$

$U_0(t)$ transforms \vec{R}_0 into \vec{R}_t while $U_{ls}(t)$ acts on the spherical harmonics present in the $\psi_l^m(\vec{r}, t)$. The result is

$$\begin{aligned} \tilde{\psi}_{\vec{R}_t}(\vec{r}) &= e^{[-i(\frac{3}{2}t + \frac{\vec{r}_t \cdot \vec{p}_t}{2}) - \frac{r^2 + r_t^2}{2} - \frac{E_0}{2}]} \\ &\times \sum_{lm} C_{lm}(\vec{R}_0) W_l(R_t r) \begin{pmatrix} (f_l + m g_l) Y_l^m(\theta, \varphi) \\ \frac{1}{2} g_l \sqrt{l(l+1) - m(m+1)} Y_l^{m+1}(\theta, \varphi) \end{pmatrix}, \end{aligned} \quad (33)$$

where $f_l(t)$ and $g_l(t)$ are simply obtained from (30) and (31) by replacing Ω by $(2l + 1)$. This expression corresponds to the most general initial condition with the assumed initial spin direction. The presence of the time dependence in the functions f and g from one hand, the presence of Y_l^{m+1} in the lower part of the spinor are the two differences which change in an appreciable manner the time evolution in the case where $\kappa \neq 0$.

We want now to concentrate our efforts on the evolution of a wave packet which is cylindrically symmetric around Oz for $t = 0$. We assume therefore (denoting unit vector in Oz direction by \hat{z})

$$\vec{r}_0 = -r_0 \hat{z}, \quad \vec{p}_0 = 0, \quad R_0 = r_0, \quad (34)$$

$$E_0 = \frac{r_0^2}{2}, \quad \theta_{R_0} = \pi, \quad \varphi_{R_0} = 0, \quad (35)$$

$$C_{lm}(\vec{R}_0) = \delta_{m0} (-1)^l 2\pi^{-\frac{1}{4}} e^{-\frac{N}{2}} \sqrt{2l+1}. \quad (36)$$

Let us study the sign of the product $C_{l0}(\vec{R}_0) Y_l^0(\theta, \varphi)$ along the Oz axis i.e. $\theta = \pi$ and $\theta = 0$. One has

$$Y_l^0(\pi, 0) = (-1)^l \sqrt{\frac{2l+1}{4\pi}} \quad (37)$$

$$Y_l^0(0, 0) = \sqrt{\frac{2l+1}{4\pi}}. \quad (38)$$

All the partial waves act coherently in the direction $\theta = \pi$ while there is a destructive interference for $\theta = 0$. We also know that there is a radial concentration of the wave packets shown on figure 2. This explains mainly the known result that the wave packet is initially a gaussian centered at $\vec{r}_0 = -r_0 \hat{z}$.

In the direction $\theta = \frac{\pi}{2}$ we have

$$Y_l^0\left(\frac{\pi}{2}, 0\right) = 0 \quad \text{if } l \text{ is odd} \quad (39)$$

while for l even its sign is $(-1)^{\frac{l}{2}}$. A destructive interference between the even states is also predicted on the xOy plane with a different character as for the $+Oz$ direction.

We will now try to repeat these arguments for $t \neq 0$ for each component of the spinor (33). For the part with $s_z = +\frac{1}{2}$ we must find the phase of the product $C_{l0} Y_l^0(\theta, \varphi) f_l(t)$. At a time $t = \frac{T_{ls}}{4} = \frac{\pi}{2}$ (assuming $\kappa = 1$) we have for high l :

$$f_l\left(\frac{\pi}{2}\right) \approx e^{i\frac{\pi}{4}} \cos(2l+1) \frac{\pi}{4} = e^{i\frac{\pi}{4}} \frac{\sqrt{2}}{2} (-1)^{\frac{l}{2}}. \quad (40)$$

The coherence of the product considered is now obtained for $\theta = \frac{\pi}{2}$ and for even l . It is interesting to see that the part with $s_z = +\frac{1}{2}$ has still cylindrical symmetry around Oz but moreover if $t = \frac{T_{ls}}{4}$ or 0 we shall have the result of figure 2 i.e. a high radial concentration of the wave. One readily understand that at this time the wave is highly peaked on a vortex of radius r_0 with symmetry around Oz , the smaller radius of the vortex being roughly the initial radial spread.

As for the part with $s_z = -\frac{1}{2}$ we must discuss the sign of the product $C_{l0} Y_l^1(\theta, \varphi) g_l(t) \times \sqrt{l(l+1)}$ also for $t = \frac{\pi}{2}$ and for $\theta = \frac{\pi}{2}$. Now $Y_l^1\left(\frac{\pi}{2}, \varphi\right) = 0$ if l is even, its sign for odd l is $(-1)^{\frac{l-1}{2}}$ while $g_l\left(\frac{\pi}{2}\right)$ has also this sign since

$$g_l\left(\frac{\pi}{2}\right) = -e^{i\frac{\pi}{4}} \frac{2i}{2l+1} \sin(2l+1) \frac{\pi}{4} = \frac{-2i}{2l+1} (-1)^{\frac{l-1}{2}} e^{i\frac{\pi}{4}} \frac{\sqrt{2}}{2}. \quad (41)$$

However we have also $Y_l^1(\theta, \varphi) \approx e^{i\varphi}$. In the case of the part with $s_z = -\frac{1}{2}$ it is the odd partial waves which produce a vortex similar to that to the part with $s_z = +\frac{1}{2}$ in the limit of high l . A difference occurs in a φ dependent phase.

For intermediate values of the time it is not possible to provide a similar discussion. However, by continuity we can understand that the vortex rings are created from the spherical initial wave packet and get their full extension for the configuration and at the time chosen.

5 Numerical simulation of the vortex rings

The manifestation of the vortex rings depends on the parameter κ . It is simpler to freeze the evolution under U_0 and to consider only the spin-orbit evolution to begin with in order to emphasize the effect. Figures 3 and 4 represent the density of the full wave packet at various times on the planes yOz and xOz , respectively. Here also we have considered the wave packet which was analyzed in figure 2. [For convenience the spin direction is $s_x = +\frac{1}{2}$

and $\vec{r}_0 = r_0 \hat{x}$ at time $t = 0$]. At time $t = 0$ a gaussian is represented. At time $t = \frac{T_{ls}}{8}$ a vortex ring has been created and gets the maximum radius at $t = \frac{T_{ls}}{4}$ when intersecting the plane yOz . Moreover figure 4 shows that even a second vortex with a smaller amplitudes has also been created that we cannot explain into simple terms. At time $t = \frac{3T_{ls}}{8}$ the vortex ring has a decreasing radius and is centered on a point with $x < 0$. Finally at time $t = \frac{T_{ls}}{2}$ the wave packet is reassembling near a point with $\vec{r}_0 = -r_0 \hat{x}$. At this time we have shown in our previous papers that the spin is approximately reversed. Finally the behaviour for $T_{ls}/2 < t < T_{ls}$ has not been shown for it is totally reversible if we assume a frozen oscillator.

The vortex rings evolve approximately on a sphere. The intersections of the wave packet with a plane xOz shown on figure 5 present indeed the feature that the distance to the center is about r_0 at all times.

The following figure 6 shows the decomposition of the toroidal wave packet into its spin components in a direction perpendicular to the classical motion. The left and central columns display the shapes of subpackets in which spin field is antiparallel and parallel to em Ox axis, respectively. Due to symmetry with respect to em Oz axis (classical trajectory), the similar decomposition with respect to spin components in an arbitrary direction perpendicular to em Oz axis results in a picture rotated by a certain angle.

6 Conclusions

The dynamics of wave packets in static potentials implies subtle interference effects which have been beautifully illustrated in the case of Coulomb potential [9-14,16]. Two general mechanisms have been identified: one is the spread of the wave on the top of a classical trajectory, the other is the regime of partial and also almost complete recurrences. In the case of a pure harmonic oscillator the existence of a single frequency allows a unique interference mechanism of the partial wave that leads to a dispersionless coherent wave packet. This is the case where quantum mechanics comes closer to classical mechanics: the dynamics of the density probability is identical to the dynamics of the density distribution of the classical ensemble. This property is expected to be lost if a perturbation is added to the potential. If the perturbation is a spin-orbit potential the dynamics of the problem resembles very much that of the JCM [24]. There exist two versions [25] of this model where the time evolution is exactly periodic in the closest analogy to our model: the Raman coupled model and the two photons JCM. In the harmonic oscillator with spin-orbit the dynamics is however richer if one follows the angular evolution with different initial conditions. We have shown previously [19] that the amount of partial revival for half a spin-orbit period depends indeed on these conditions. We have discussed extensively [18, 21] cases where the wave packet is divided into two parts which rotate in opposite directions on a circular average

trajectory in much the same way as the Stern-Gerlach effect. In the present paper we have shown a new dynamical behaviour for cylindrically symmetric initial conditions: vortex rings are created and destroyed periodically. In a way this is a case where the coherence of the wave is kept for the r and θ coordinates but where the spread is applied only to the ϕ variable. It is an open question whether this effect relies only on the properties of the partial waves of the harmonic oscillator discussed in this paper.

Acknowledgements

One of us (P R) likes to express his thanks to ISN, Grenoble for kind hospitality during his stay in June–July 1996, when much of work have been done.

References

- [1] Alber G and Zoller P 1991 *Phys. Rep.* **199** 231.
- [2] Garraway B M and Suominen K-A 1995 *Rep. Prog. Phys.* **58** 365.
- [3] Jaynes E T and Cummings F W 1963 *em Proc. IEEE* **51** 129.
- [4] Buck B and Sukumar C V 1981 *em Phys. Lett. A* **81** 132.
- [5] Knight P L 1986 *em Phys. Scripta T* **12** 51.
- [6] Gea-Banacloche J 1990 *em Phys. Rev. Lett.* **65**;
1991 *Phys. Rev. A* **44** 5913;
1992 *Opt. Commun.* **88** 531.
- [7] Averbukh I S 1992 *Phys. Rev. A* **46** R2205.
- [8] Brown L S 1973 *Am. J. Phys.* **41** 525.
- [9] Parker J and Stroud C R Jr. 1986 *Phys. Rev. Lett.* **56** 716.
- [10] Averbukh I S and Perelman N F 1989 *Phys. Lett. A* **139** 449;
1989 *Zh. Eksp. Teor. Fiz.* **96** 818 (1989 *Sov. Phys JETP* **69** 464);
1991 *Usp. Fiz. Nauk* **161** 41 (1991 *Sov. Phys Usp.* **34** 572).
- [11] Dačić-Gaeta Z and Stroud C R Jr. 1990 *Phys. Rev. A* **42** 6803.
- [12] Peres A 1993 *Phys. Rev. A* **47** 5196.
- [13] Wals J Fielding H H and van Linden van den Heuvell H B 1995 *Physica Scripta T* **58** 62.
- [14] Bluhm R and Kosteletzky V A 1995 *Phys. Lett. A* **200** 308.
- [15] Abramowitz M and Stegun I A 1964 *Handbook of Mathematical Functions* (National Bureau of Standards) sect.10.2.
- [16] Boris S D Brandt S Dahmen H D and Stroh T 1993 *Phys. Rev. A* **48** 2574.
- [17] Cohen-Tannoudji Diu C B and Laloe F 1977 *Mécanique Quantique* (Paris: Herman) p.570.
- [18] Arvieu R and Rozmej P 1994 *Phys. Rev. A* **50** 4376.
- [19] Arvieu R and Rozmej P 1995 *Phys. Rev. A* **51** 104.

- [20] Rozmej P and Arvieu R 1996 *J. Phys.* B **29**1339.
- [21] Rozmej P and Arvieu R 1996 *Acta Phys. Polon.* B **27** 581.
- [22] Rozmej P Berej W and Arvieu R em invited talk at XXXI Zakopane School of Physics, September 3–11, 1996, [to appear in *Acta Phys. Polon. A* (1997)].
- [23] Mikhajlov V V 1973 *Izv. Akad. Nauk SSSR, Ser. Fiz.* **37** 2230 (1974 *Bull. Acad. Sci. USSR, Phys. Ser.* **37** 187).
- [24] Shore B W and Knight P L 1993 *J. of Modern Optics* **40** 1195.
- [25] Phoenix S J D and Knight P L 1990 *J. Opt. Soc. Am.* B **7** 116.

Figure captions

- Fig. 1.** Radial motion of eight lowest partial waves with $l = 0, 1, \dots, 7$ contributing to the linear motion of the gaussian wave packet. Shown is $|r\psi_l(r, t)|^2$ as a function of r for 30 time steps in the interval $t \in [0, \frac{T}{2}]$. The case $E_0 = N = 20$ is presented. The vertical scale is the same for all figures.
- Fig. 2.** Decomposition of the gaussian wave packet into partial waves at $t = 0, r_0 = \sqrt{2N} = \sqrt{40}$. The lowest 16 partial waves with $l = 0, 1, \dots, 15$ are shown. Waves with $l = 0 - 4$ are represented by solid lines (intensity increases with l), those with $l = 5 - 15$ by dashed ones (their intensities decrease).
- Fig. 3.** Time evolution of the wave packet with spin under $U_{ls}(t)$ operator only (evolution according to U_0 is frozen). Shown is the $|\Psi(t)|^2 = |\Psi_+(t)|^2 + |\Psi_-(t)|^2$ as a function of coordinates on the plane xOz . Case $N = 20$. Note different vertical scales. Cases em a,b,c,d,e,f correspond to $t_i = 0, 1/8, 2/8, 3/8, 15/32$ and $4/8 T_{ls}$ respectively.
- Fig. 4.** The same wave packet as in previous figure. Here shown are cuts through planes perpendicular to the classical trajectory (em Oz axis) with $z_i = z_0 \cos t_i$ showing explicitly a toroidal shape. Time instants as in previous figure.
- Fig. 5.** Contour plots of the same evolution as in figure 4, showing that centers of the vortex rings evolve approximately on a sphere with the radius r_0 . Here packets corresponding to different time instants are collected in the same picture.
- Fig. 6.** Contour plots showing the decomposition of the total wave packet (right column) into parts with the opposite spin field (left and central columns). Case $N = 4$. Top row a) corresponds to $t = 0$, bottom e) to $t = \frac{1}{2}T_{ls}$. Time steps are $\Delta t = \frac{1}{8}T_{ls}$.

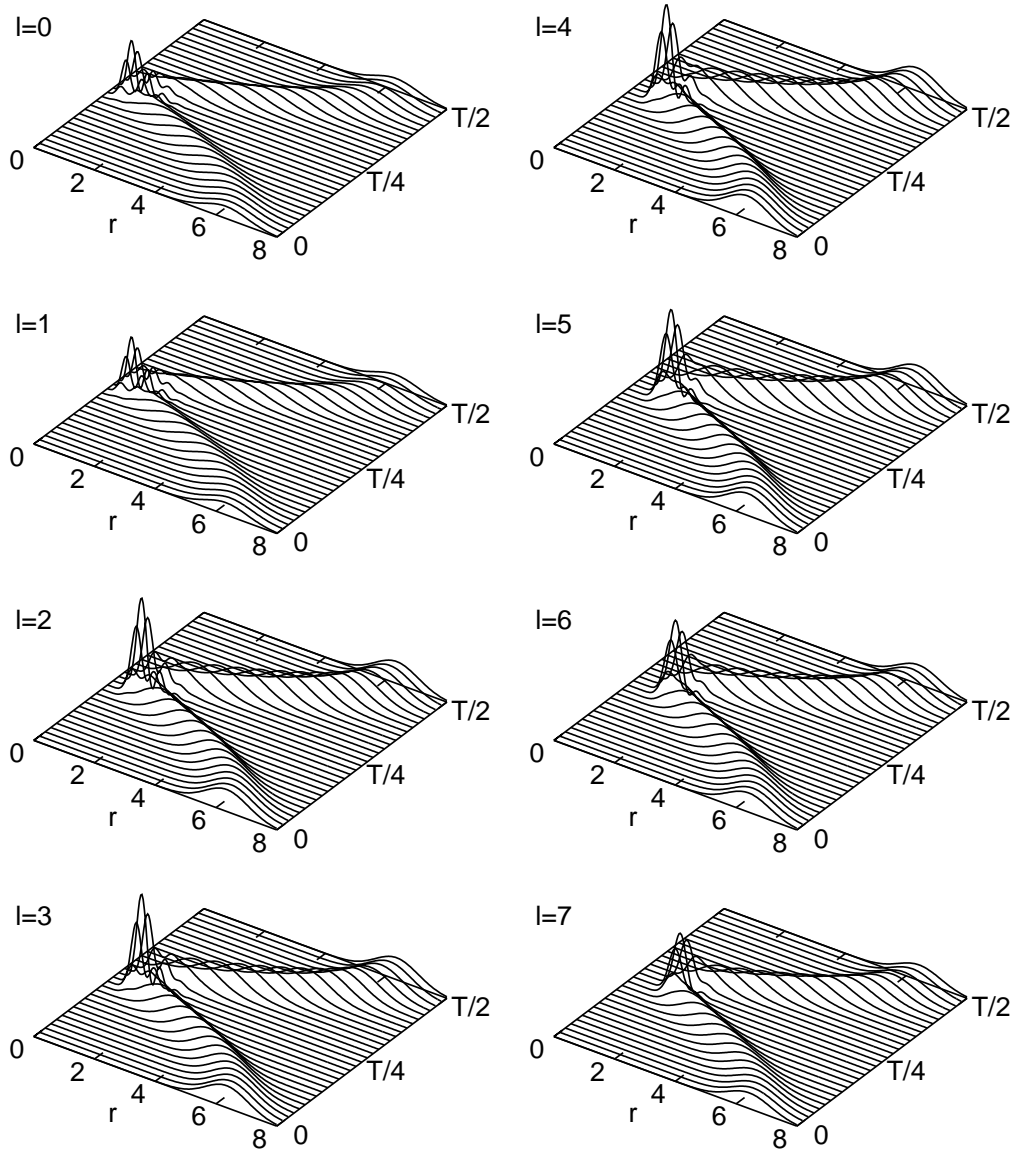


Figure 1. Radial motion of eight lowest partial partial waves with $l = 0, 1, \dots, 7$ contributing to the linear motion of the gaussian wave packet. Shown is $|r\psi_l(r,t)|^2$ as a function of r for 30 time steps in the interval $t \in [0, \frac{T}{2}]$. The case $E_0 = N = 20$ is presented. The vertical scale is the same for all figures.

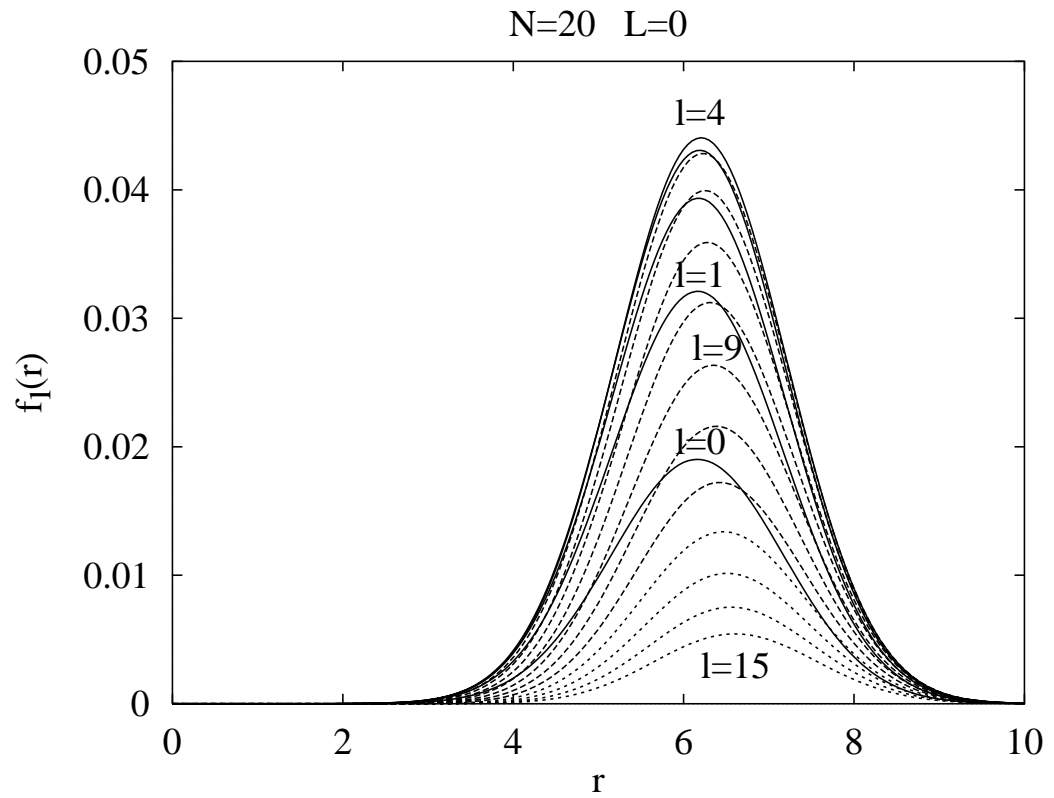


Figure 2. Decomposition of the gaussian wave packet into partial waves at $t = 0$, $r_0 = \sqrt{2N} = \sqrt{40}$. The lowest 16 partial waves with $l = 0, 1, \dots, 15$ are shown. Waves with $l = 0 - 4$ are represented by solid lines (intensity increases with l), those with $l = 5 - 15$ by dashed ones (their intensities decrease).

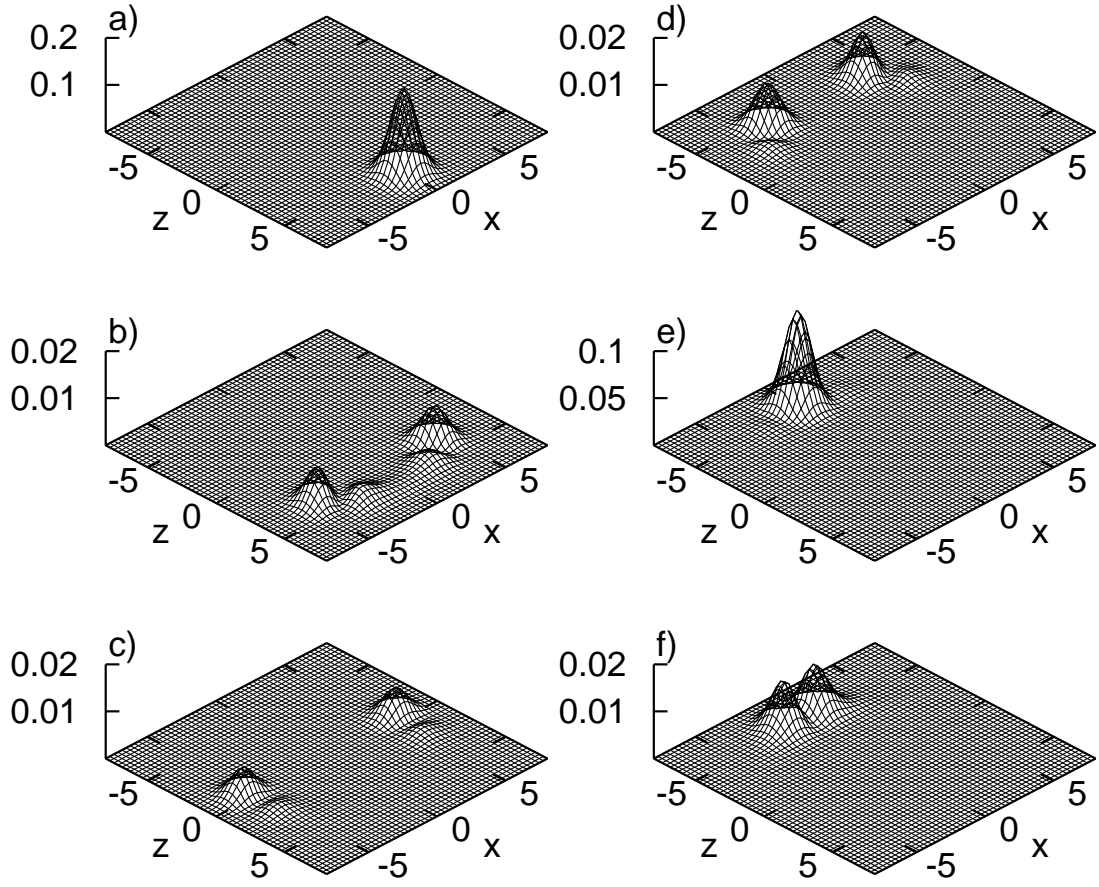


Figure 3. Time evolution of the wave packet with spin under $U_{i_s}(t)$ operator only (evolution according to U_0 is frozen). Shown is the $|\Psi(t)|^2 = |\Psi_+(t)|^2 + |\Psi_-(t)|^2$ as a function of coordinates on the plane xOz . Case $N = 20$. Note different vertical scales. Cases a, b, c, d, e, f correspond to $t_i = 0, 1/8, 2/8, 3/8, 15/32$ and $4/8 T_{i_s}$ respectively.

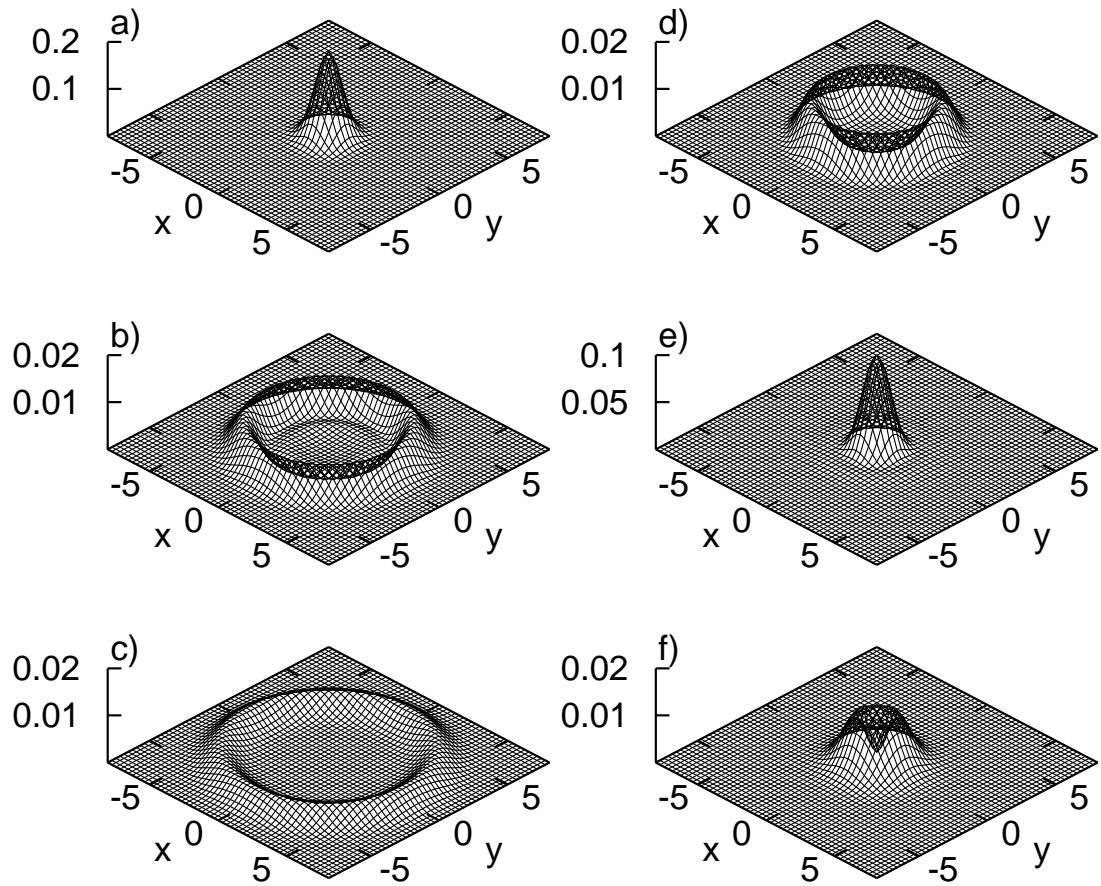


Figure 4. The same wave packet as in previous figure. Here shown are cuts through planes perpendicular to the classical trajectory (Oz axis) with $z_i = z_0 \cos t_i$ showing explicitly a toroidal shape. Time instants as in previous figure.

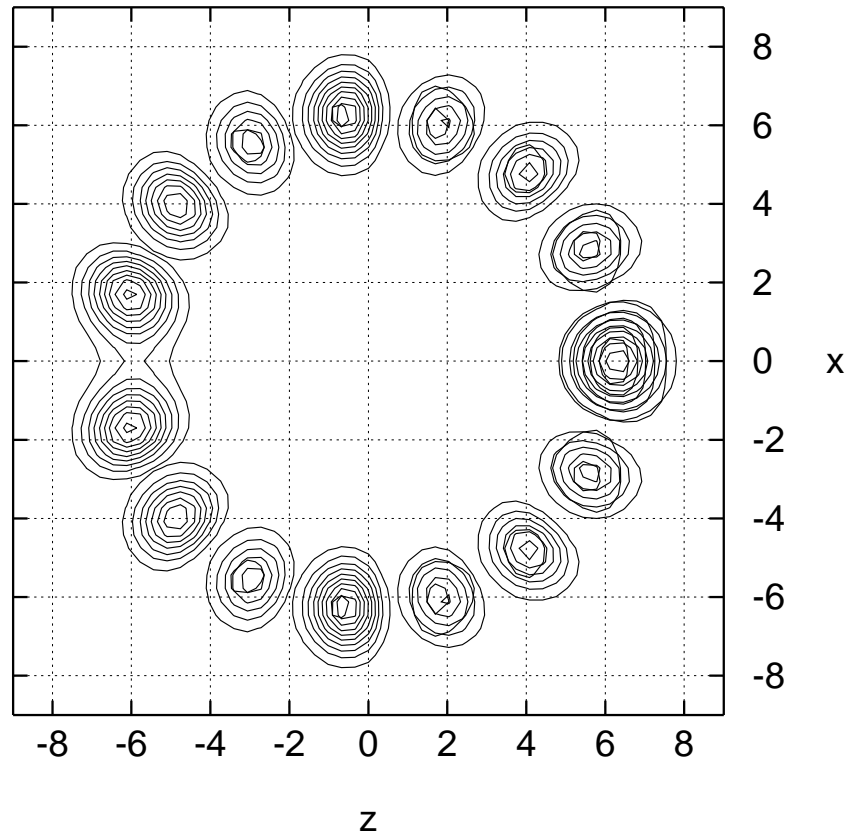


Figure 5. Contour plots of the same evolution as in figure 4, showing that centers of the vortex rings evolve approximately on a sphere with the radius r_0 . Here packets corresponding to different time instants are collected in the same picture.

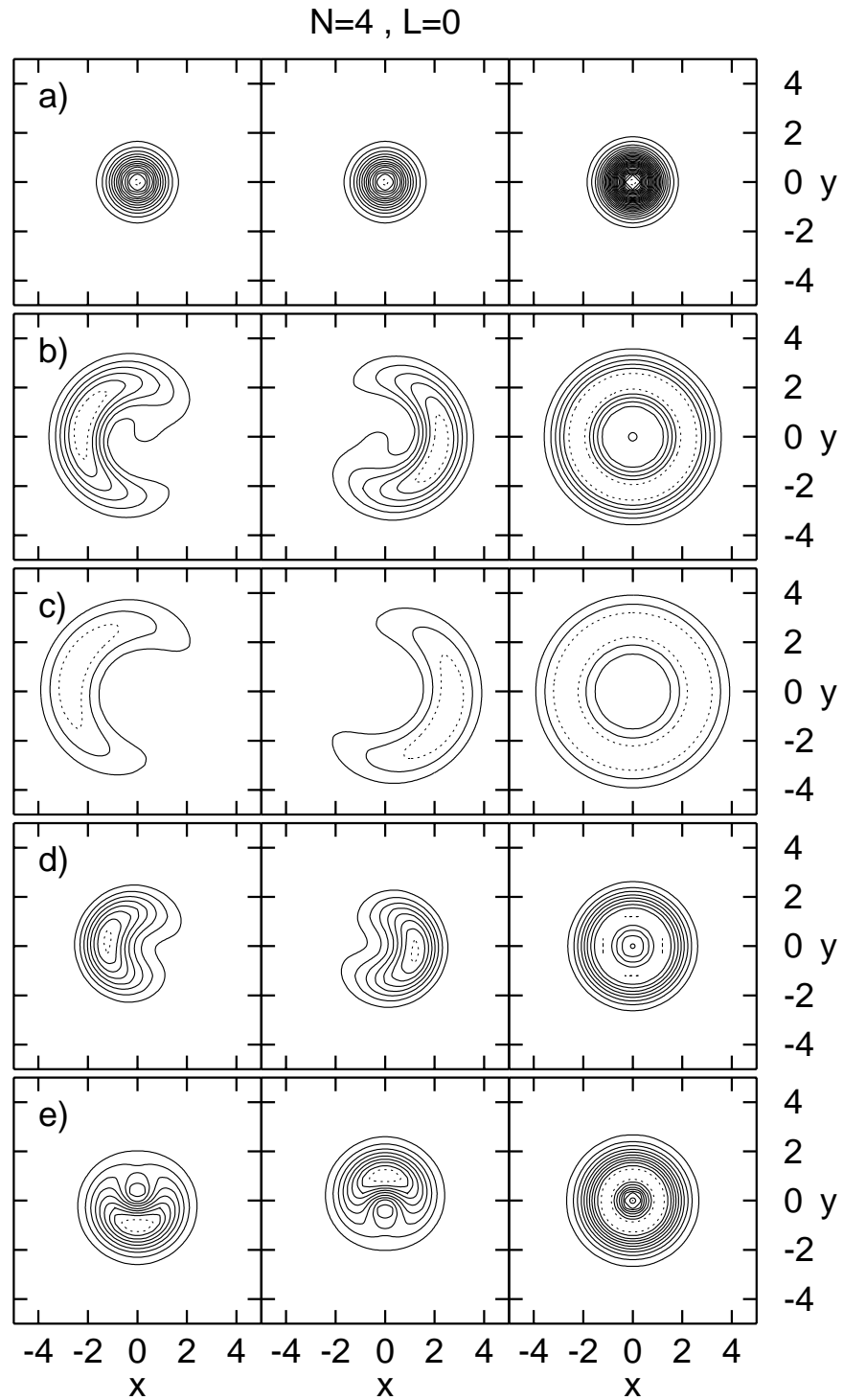


Figure 6. Contour plots showing the decomposition of the total wave packet (right column) into parts with the opposite spin field (left and central columns). Case $N = 4$. Top row a) corresponds to $t = 0$, bottom e) to $t = \frac{1}{2}T_{ls}$. Time steps are $\Delta t = \frac{1}{8}T_{ls}$.